ACS OMEGA

Open Access

This article is licensed under CC-BY-NC-ND 4.0

http://pubs.acs.org/journal/acsodf

Article

Cure Kinetics and Thermal Behavior of a Printable Polydimethylsiloxane-Based Polymer

Cody Cockreham,* John Rosener, Steven A. Hawks, and Elizabeth Glascoe

Cite This: *ACS Omega* 2025, 10, 10294−10301

Read Online

ACCESS | Metrics & More | Article Recommendations | Supporting Information

ABSTRACT: In this study, we investigate the curing reaction kinetics and degree of cross-linking of LL50, a polydimethylsiloxane (PDMS)-based polymer, using isothermal heat flow calorimetry (HFC). LL50, developed by Lawrence Livermore National Laboratory, is a two-part addition-curing liquid silicone rubber for direct-ink-writing additive manufacturing. The curing process, driven by a platinum-catalyzed hydrosilylation reaction, was monitored under isothermal conditions at various temperatures. We developed a kinetic model to predict the curing rate and extent of the reaction. The model was validated within the temperature range of 50 to 80 °C, showing good agreement with experimental data. However, the model's extrapolation to near-room temperatures (30 °C) was less accurate, indicating that different kinetic mechanisms may be at play. Our findings highlight the importance of validating kinetic models across relevant temperature ranges and underscore the utility of isothermal calorimetry in studying polymer curing processes. This study provides insights into the processing conditions necessary for the optimal performance of LL50 in 3D printing applications.

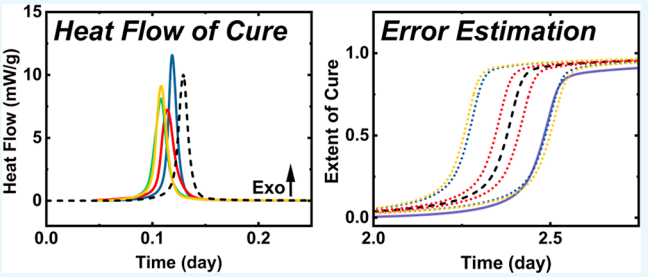

INTRODUCTION

Silicone rubbers are used in various applications due to their unique properties such as good thermal, oxidative, and mechanical stabilities, biocompatibility, tunable optical properties, flexibility, and reliability over a range of temperatures and humidity.[1−6] These qualities make them suitable for emerging technologies such as soft robots, shock-absorption devices, engineered foam structures, and biocompatible materials. Additionally, silicone polymers are well-suited for 3D printing due to their shear-thinning and easy-curing qualities, allowing the creation of unique and complex polymer structures with low total volume density.[7,8]

Recently, Lawrence Livermore National Laboratory (LLNL) developed a polydimethylsiloxane (PDMS)-based copolymer containing a surface-treated silica filler (LL50) for use in direct-ink-writing (DIW) additive manufacturing (i.e., 3-dimensional, or 3D, printing).[9−12] It is a two-part, addition-curing liquid silicone rubber. LL50 is exothermically solidified through cross-linking hydrosilylation reactions.[13] This reaction involves the addition of a silicon−hydrogen (Si−H) bond across a carbon−carbon double bond (C═C), typically a vinyl group, in the presence of a platinum catalyst, most commonly Karstedt's catalyst.[14,15] The reaction mechanism begins with the activation of the platinum catalyst, which facilitates the formation of a reactive intermediate complex between the Si−H group and the vinyl group. This complex undergoes a transition state where the Si−H bond is cleaved and the silicon atom forms a new bond with the carbon atom of the vinyl group, resulting in the formation of a Si−CH_2−CH_2−Si linkage. The reaction is highly exothermic, releasing heat energy that can be monitored calorimetrically. The presence of an inhibitor is often necessary to control the reaction rate and prevent premature curing at room temperature. The reaction is thermally driven; the pot life and cure time depend on processing temperatures.

LL50 is designed to be cured by following 3D printing. It is critical to avoid curing during processing or storage because thickening may occur, which could translate into poor printing performance. 3D printing applications may require an extended pot-life at near-room temperature for printing large parts. To predict the pot-life of a batch of LL50 material, we developed a kinetic model using isothermal calorimetry. The heat release from the polymer cross-linking reaction can be used to monitor the curing process in situ.[16,17] Isothermal heat flow calorimetry (HFC) is an ultrasensitive (∼100 s of nW) microcalorimetric technique allowing heat flux measurements over extended durations (days to years) with high integral heat accuracies. HFC is uniquely suited to measuring the slow curing behavior of PDMS-based polymers at near-room temperature. Here, we monitor the curing behavior under

Received: October 29, 2024
Revised: January 6, 2025
Accepted: January 13, 2025
Published: March 6, 2025

ACS Publications

© 2025 The Authors. Published by American Chemical Society

isothermal conditions and develop a simple kinetic model to predict the curing rate.

SAMPLE AND EXPERIMENTAL METHODS

Materials. The siloxane copolymer developed at LLNL is designated as Llama50 (LL50).[9] LL50 is prepared in two parts and mixed mechanically. Part A contains Nusil PLY3-7560 [10,000 cSt poly(dimethyl)-co-(diphenyl)siloxane, vinyl terminated] at 66.99 wt %, Aerosil R8200 (hexamethyldisilazane-treated fumed silica) at 32.16 wt %, Elkem Bluesil Thixo Add 22646 at 0.27 wt %, and a platinum−palladium catalyst blend of Nusil PLY2-7560 [1000 cSt poly(dimethyl)-co-(diphenyl)-siloxane, vinyl terminated] and Karstedt catalyst at a mass ratio 9:1 at 0.58 wt % for 13.1 ppm Pt. Part B contains Gelest HMS-H271 [poly(hydromethyl)-co-(dimethylsiloxane), dimethylhydrosilane terminated] at 45 wt %, Gelest DMS-V05 [6 cSt poly(dimethylsiloxane)] at 27 wt %, Nusil PLY3-7560 at 22 wt %, and an inhibitor blend containing 1-ethynyl-1-cyclohexanol at 6 wt % and 6000 ppm 1-ethynyl-1-cyclohexanol. Parts A and B are mixed in ratios of 10:1. Each sample was mixed in three cycles at 1400 rpm for 30 s for each spin in a FlackTek mixer and hand mixed with a spatula in between mixing spins. The sample was exposed to room temperature for 2 h before being placed in a freezer. The sample was removed from the freezer and was exposed to ∼3 h of room temperature prior to data being collected on any given technique in this study. Discussed in the text, the sample is curing slowly during this wait time at room temperature. The possible effect of room temperature exposure is discussed below.

Thermogravimetric Analysis. Thermogravimetric analysis (TG) was performed using a TA Instruments first generation Discovery system running TRIOS software V5.7.0.14. Testing conditions involved a heating rate of 10 °C/min and a nitrogen purge flow rate of 25 mL/min. Sample mass of 3.8 mg was analyzed in a 100 μL platinum pan from 30 to 600 °C.

Differential Scanning Calorimetry. Differential scanning calorimetry (DSC) was performed on a TA Instruments Q2000 system running TA Advantage software V24.11. Testing conditions involved a heating rate of 10 °C/min and a nitrogen purge flow rate of 50 mL/min. About 12 mg of the sample was analyzed in a Tzero aluminum crucible from 30 to 200 °C.

Isothermal Calorimetric Analysis. Isothermal calorimetry was performed by using a TA Instruments Thermal Activity Monitor (TAM III). Instrument baseline is measured prior to and following the measurement. Experimental details including the date of the start of the measurement, temperature of measurement, mass of sample, calorimeter type, and ampule is cataloged in Table S1. Briefly, the experiments used two different sized stainless-steel vials (4 and 20 mL), with sample masses ranging from approximately 98 to 903 mg, in three different calorimeters (i.e., TAM III "4 mL nanocalorimeter", "20 mL microcalorimeter", and "20 mL multicalorimeter") with slightly different sensitivities. The variation in sample mass, calorimeter, and vial is analyzed and discussed below.

Insertion of the sample into the calorimeter requires heating to acclimate the temperature of the vessel for 15 min before the heat flux is measured. Calorimeter accuracy was measured to be within ±1.5% of the theoretical enthalpy of melting for a biphenyl standard. Error was estimated to be two standard deviations of the mean. The kinetic model was derived using AKTS Thermokinetics software, which in turn uses an isoconversional method discussed further below.[18]

RESULTS AND DISCUSSION

DSC was performed on uncured LL50 (see Figure 1). DSC measured an exotherm with a peak at ∼126 °C, assigned to

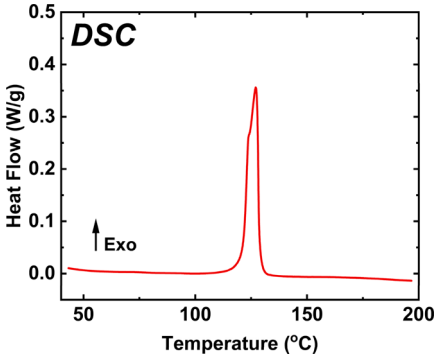

Figure 1. Differential scanning calorimetry (DSC) of LL50 conducted at 10 °C/min.

cross-linking reactions. TG measures ∼0.5 wt % between 100 to 200 °C, attributed to water/solvent loss and volatile products of curing, presented in Figure S1. We do not believe that the mass loss is related to the curing process. No significant decomposition or endothermic reaction, such as pyrolysis, was observed in either the TG or DSC up to 200 °C. Thermal stability of PDMS and poly(dimethyl diphenyl siloxane) copolymers is expected in this temperature range.[19,20] Karstedt's catalyst requires oxygen to perform hydrosilylation reactions; however, due to the mobility of oxygen and the low sample mass, we expect that the diffusion of oxygen is not limiting.[21,22] These initial results indicate that calorimetry is well-suited to study the cross-linking of LL50.

Isothermal calorimetric measurements were used to monitor the curing of LL50. Heat flow curves as a function of time are presented in Figure 2. Four measurements were performed at each of the following temperatures: 50, 60, 70, and 80 °C. However, at 50 °C, one measurement returned an integrated heat of less than two-standard deviations of the mean. This outlying measurement was treated as an anomaly and was not included in the data analysis. Heat flow shows an exothermic peak produced from cross-linking through hydrosilylation of vinyl and hydride end blocked groups. Integral heats of reaction or "heats of cure" were determined by integrating across the exothermic heat flow peak using a sigmoidal baseline. All integrations are presented in Figures S2−S16. A sigmoidal baseline is justified by the expected change in the heat flow baseline due to the decrease in heat capacity from a decrease in entropy, as cross-linking reduces the degrees of freedom of polymer chains. Error was estimated to two-standard deviations of the mean; no significant difference in integral heats measured at different temperatures was evidenced. The heat of cure was determined to be −12.03 ± 0.58 J/g (n = 15). There is no noticeable trend in the specific heat of cure mass of sample from a near-zero slope of a linear fit of the data with poor correlation (Figure S17). Additionally, the heat of cure displays no dependence on the temperature of measurement; all averaged heats of cure at temperature of measurement are within error (Figure S18).

https://doi.org/10.1021/acsomega.4c09881
ACS Omega 2025, 10, 10294−10301

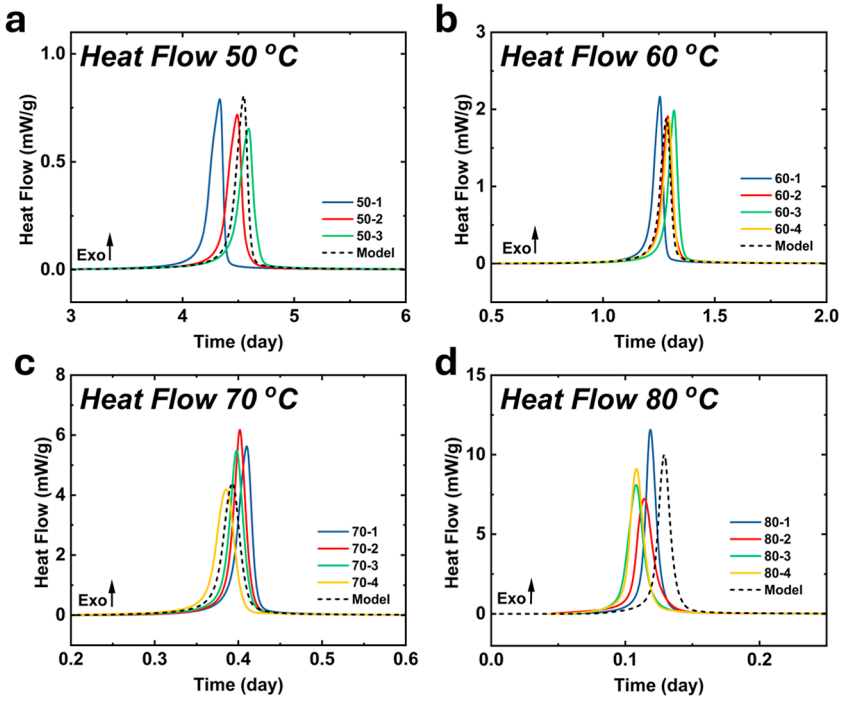

Figure 2. Mass normalized heat flow as a function of time in isothermal LL50 in situ curing measurements performed at temperatures of (a) 50, (b) 60, (c) 70, and (d) 80 °C. Measured data are presented as solid lines and the kinetic model fit is presented as a dashed line.

Using Hess's Law and average bond energies retrieved from literature, an estimation can be made for the energy of each cross-linking reaction.[23,24] The energy required to break the Si−H and C═C bonds is estimated by eq 1.

$$\Delta H_{\text{broken}} = 393\ (\text{Si} - \text{H}) + 614\ (\text{C\&\#xe5fb; C})\ \frac{\text{kJ}}{\text{mol}} = 1007\ \text{kJ/mol} \quad (1)$$

The energy released by the formation of the Si−CH_2−CH_2−Si chain is estimated by eq 2.

$$\Delta H_{\text{formed}} = -432\ (\text{H} - \text{H}) + - 347\ (\text{C} - \text{C}) + - 360\ (\text{Si} - \text{C})\ \frac{\text{kJ}}{\text{mol}} = -1139\ \text{kJ/mol} \quad (2)$$

The net energy of the reaction is calculated by summation in eq 3.

$$\Delta H_{\text{net}} = \Delta H_{\text{broken}} + \Delta H_{\text{formed}} = -132\ \text{kJ/mol} \quad (3)$$

This analysis provides theoretical support for the notion that the hydrosilylation reaction is exothermic with an estimated reaction energy of −132 kJ/mol. Using the bond energies of the unique molecules instead of average bond energies would be more accurate, but for the purpose of qualification, we find this analysis sufficient. Without a well-defined molecular weight, which is difficult to ascertain, we cannot directly compare the measured heat of cure and the estimated enthalpy of the hydrosilylation reaction.

The progress of the curing reaction, sometimes referred to as the extent of reaction (α), was derived by dividing the current heat by the total heat of reaction and plotted as a function of time in Figure 3a. Rate of reaction, i.e., ($d\alpha/dt$), is analogous to measured heat flow. From the assumptions listed, a model-free isoconversional method can be used to determine the kinetic parameters as the apparent energy of activation is dependent on the extent of reaction. The fits of the model compared to example data of the measured heat flow (i.e., rate of cure or $d\alpha/dt$) are also presented in Figure 2a−c. The model fits are in good agreement with the data. The fits fall within the distribution of α for all points of time for measurements at 50, 60, and 70 °C. At 80 °C, the model predicts peak heat flow and α to be at longer times than the measurements evidence (Figures 2d and 3a.) This is due to the sample being inserted into the calorimeter in a preheating location for ∼15−20 min before being placed into measurement position. This is standard experimental procedure with the TAMIII instrumentation to avoid thermal shock, but curing occurs rapidly (within hours) at 80 °C. The sample starts curing immediately, and the heat signal is not recorded during this initial preheating step. We expect that if this heat signal were to be recorded at 80 °C, the measurement and model fit would be in similar agreement to that seen in measurements at lower temperatures. While some degree of curing is unrecorded during this preheating time for measurements at lower temperatures, ∼15−20 min is negligible.

The energy of activation is determined by producing isoconversional lines with the reaction rates versus temperature by the simple manipulation of Arrhenius kinetics. AKTS software utilizes a differential isoconversional method to determine the kinetic parameters. The isoconversional method is a simple technique to directly incorporate possible multistep reactions into a model. A rigorous explanation on how the differential isoconversional method is employed in the software is available from AKTS.[18,25] Briefly, the differential isoconversional method is based on eq 4.

$$\ln\left(\frac{d\alpha}{dt}\right)_{\alpha,i} = \ln\left(f(\alpha)A_\alpha\right) - \frac{E_\alpha}{RT_{\alpha,i}} \quad (4)$$

https://doi.org/10.1021/acsomega.4c09881
ACS Omega 2025, 10, 10294−10301

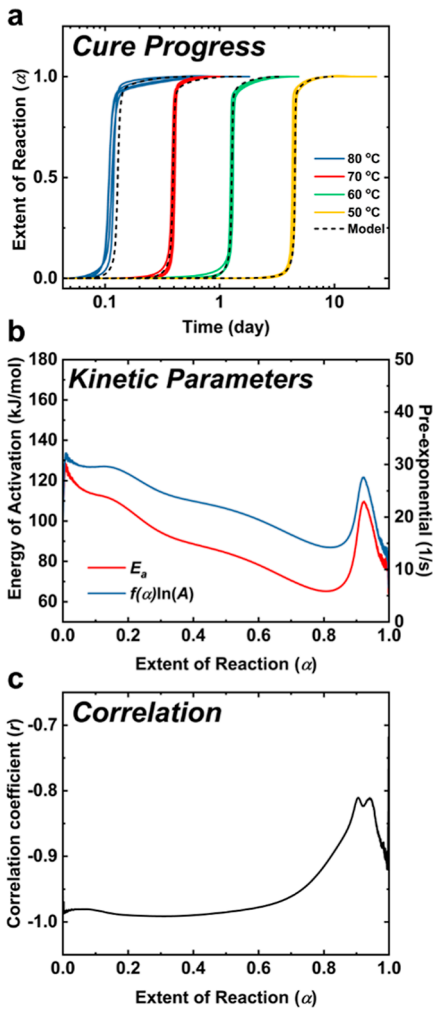

Figure 3. (a) Cure progress presented as a function of time from isothermal calorimetry measurements and fitted parameters. (b) Kinetic parameters, energy of activation (E_a) and pre-exponential term, combined pre-exponential factor and reaction model [$f(\alpha)$ ln (A)] as a function of the extent of reaction (α) as determined by AKTS Software employing differential isoconversional analysis method. (c) Correlation coefficient (r) of the fit as a function of extent of reaction.

where E_α is the energy of activation, R is the ideal gas constant, and the index i denotes the various temperatures at which the measurements were performed. The E_α is determined from the rate of change (or slope) of the left-hand side of eq 4 (LHS) vs $1/T_\alpha$. $f(\alpha)$ A_α is the kinetic model and pre-exponential factor. Differential isoconversional analysis avoids the assumption of a kinetic model by grouping the $f(\alpha)$ A_α terms and determining their combined values at every step of analysis. The product of the $f(\alpha)$ A_α is determined from the intercept of LHS vs $1/T_\alpha$. The derived energy of activation and $f(\alpha)$ A_α as a function of reaction progress is presented in Figure 3b. The $f(\alpha)$ A_α mirrors the energy of activation because of the kinetic compensation effect, an intrinsic linear relationship between the pre-exponential factor and activation energy.[26] We interpret the energy of activation to display a general decrease involving three steps and finally an increased peak at high extents of reaction. Previously discussed in literature, the hydrosilylation reaction occurs in three stages: (1) an induction period in which the Karstedt's catalyst must undergo hydrosilylation or exchange of ligands prior to hydrosilylation of the added olefin, (2) a hydrosilylation reaction of the Si−H and C═C groups, and (3) a "post-cure" reaction of remaining cross-linking groups.[21,27] Common practice ignores the first and last 10% of isoconversional analysis kinetics. We limit our interpretation to the domain of $0.1 < \alpha < 0.9$. The initial stage up to $\alpha = 0.2$ (E_α = > 100 kJ/mol) likely accounts for the induction period. The second stage occurring between $\alpha = 0.2$ to 0.6 (E_α = 80−100 kJ/mol) can be attributed to the hydrosilylation reaction, cross-linking the hydride and vinyl terminated chains. The third stage is a decrease to E_α = 60−80 kJ/mol from α = 0.6 to 0.9 and is attributed to a small-molecule diffusion-controlled mechanism. A diffusion-controlled mechanism is commonly observed in isoconversional analysis using isothermal techniques in polymer cross-linking.[17] The coefficient of correlation, the r value, is presented in Figure 3c and represents the agreement of the measured reaction progress and isoconversional fit. The fit agrees well with the measured data at $\alpha < 0.7$, having an $r > -0.95$. There is less correlation between the fit and data at higher extents of reaction ($\alpha > 0.7$). The decrease in correlation mirrors the transition out of chemical reaction-controlled kinetics into diffusion-controlled mechanisms, including the locking of the unbranched chains. The model struggles to describe this diffusion behavior in the polymer. This may be due to natural variation in the curing process or even temperature-related effects.

Previously, the energy of activation for the cross-linking curing reaction of several PDMS-based polymers has been reported. Generally, the differences in the energies of activation reflect the differences in the composition of the PDMS and testing methodology. Hong and Lee report E_α = 103−109 kJ/mol for Silbione LSR 4330.[28] The energies were determined by using a variety of integral and differential isoconversional methods from DSC measurements. This corresponds well to the induction period energies of activation measured at the initial stages of curing. Harkous et al. calculated from differential isoconversional analysis of DSC to be ∼74 kJ/mol for Silbione LSR 4350 HC.[29] This compares to the measured region of the third stage of our energies, which displays a diffusion-controlled mechanism. Bardelli et al. report energies of activation as a function of extent of reaction calculated from differential isoconversional methods applied to rheological, isothermal, and dynamic calorimetric data.[30] Isothermal and dynamic calorimetric techniques produce E_α = 80−100 kJ/mol for α = 0 to 0.6. These energies correspond to the measured hydrosilylation reactions of the Si−H and C═C groups. Bardelli et al. also observes a decrease in E_α at α = > 0.6 corresponding to a diffusion-controlled mechanism. Rheological characterization calculated E_α = ∼ 60−75 kJ/mol for α = 0 to 0.6. It has been observed that heat release can be detected without mechanical change to a material behavior, which could account for the lower energies of activation measured by rheology. Compared to Sylgard-184, a slower reaction rate (and therefore higher curing temperatures) is observed for LL50. We expect the higher activation energies of LL50 to be due to the presence of the cure inhibitor, 1-ethynyl-1-cyclohexanol.

To assess the kinetic model's performance within the 50−80 °C range, we conducted a curing measurement at 55 °C. This measurement was not part of the initial model fitting, allowing for an independent evaluation of the model's accuracy at this specific temperature. Our analysis of the model's predictive accuracy at 55 °C incorporates error analysis techniques

https://doi.org/10.1021/acsomega.4c09881
ACS Omega 2025, 10, 10294−10301

detailed below. We selected 55 °C because it is at the lower end of the temperature range studied, making it more relevant to typical storage conditions compared to higher temperatures such as 65 or 75 °C. The model predicts a faster reaction rate than what is measured by calorimetry. The measured and simulated exotherms have a peak maximum difference of ∼0.11 days. Regarding shape, the measurement has a longer tail on the right side of the exotherm and near $\alpha = 1$ in the extent of the reaction curve. To assess the agreement, we perform an error analysis of the model.

Heat flow (a) and extent of reaction (b) from isothermal calorimetry measurements and fitted parameters of LL50 curing at 55 °C.

To assess the variability and sensitivity of our kinetic model to the variability of the data, we developed kinetic models using limited sets of measurements. We performed Bootstrap Monte Carlo analysis as well as varied the measurements that were incorporated into the analysis based on the temperature and calorimeter type. In Figure 5a, predictions of LL50 curing at 55 °C is presented using 10 measurements resampled 10 iterations. The data used in each prediction are detailed in the Supporting Information. To compare the Bootstrap analysis with our initial model, that incorporates all 15 measurements, we use time to reach $\alpha = 0.5$ ($t_{0.5}$) at 55 °C. The all-data model has $t_{0.5}$ = 2.377 days and bootstrap analysis returns a $t_{0.5}$ = 2.377 ± 0.033 days (n = 10, error = 1.37%). Error was determined from two-standard deviations of the mean. From our 10 bootstrap samplings, we found that the model has an estimated error of 1.37%.

To determine the influence of measurement temperature on the model, we developed the model by excluding each of the temperature sets once. This is presented in Figure 5b. Simulations without 60, 70, and 80 °C (No60C, No70C, and No80C) are in strong agreement with each other; differences are negligible, $t_{0.5}$ = 2.365 ± 0.006 days (n = 3, error = 0.23%). The simulation excluding the 50 °C (No50C) has $t_{0.5}$ = 2.474 days, which is ∼0.11 days different than the other predictions and actually much closer to the measured data $t_{0.5}$ = 2.483. We find that the measurements done at 50 °C have a strong influence on the predictions of a simulated cure at 55 °C. Measurements at 50 °C were performed last out of the measurements used in the model, meaning the samples used were exposed to room temperature the most (at least 4 times since mixing) and have been stored the longest. This could explain the apparent influence of 50 °C on faster predicted reaction rates. Simulations from varied temperature sets return a $t_{0.5}$ = 2.392 ± 0.109 days (n = 4, error = 4.58%).

Measurements were performed in different calorimeter types or "channels" in the TAMIII. Measurements were performed in a 4 mL volume calorimeter channel branded a "Nanocalorimeter" by TA and 20 mL calorimeters "Microcalorimeter" and "Multicalorimeter" channels. We discuss what we believe to be the relevant differences from the measurements. In Figure 5c, we present simulations that are modeled using data from sets excluding one or more of the calorimeter types to determine the influence of calorimeter type on the model. There are 5 simulations: No4mlNano describes the model that used all of the data sets except measurements performed in the 4 mL "Nanocalorimeter", No20mLMicro excludes the 20 mL "Microcalorimeter", No20mLMulti excludes the 20 mL "Multicalorimeter", Only4mLNano includes only 4 mL "Nanocalorimeter", and Only20mLMulti includes only 20 mL "Multicalorimeter" measurements. Calorimeter channel type plays a significant role in the prediction of the cure. Comparing the fastest simulation (Only4mLNano) $t_{0.5}$ = 2.304 days to the slowest (Only20mLMulti) $t_{0.5}$ = 2.462 days, a difference of ∼0.15 days is found. This is almost certainly due to the differences in heat transfer lengths of the two calorimeter types. First, the 20 mL ampules have at least 5× larger thermal mass than the 4 mL ampules by weight of the ampules. Second, curing of LL50 was performed inside metal crucible liners placed in 4 mL metal ampules and in glass liners inside 20 mL metal ampules. Heat transfer is slower out of the 20 mL ampule. Third, we commonly added more mass of LL50 into the larger ampules (see Table S1), which could add heat transfer length. This analysis shows just how much influence the experimental setup can have on calorimetric results. Simulations of varied calorimeter types have a $t_{0.5}$ = 2.378 ± 0.122 days (n = 5, error = 5.12%).

The calculated errors from our simulation analyses are used to estimate the error in the simulation of the model incorporating all of the calculated errors at 55 °C in Figure 5d. Analyzed this way, the measurement and simulation are in decent agreement, having $t_{0.5}$ within the estimated errors determined from the temperature variation (4.58%) and calorimeter type variation (5.12%) analyses. It is notable that the measurement is outside of the estimated errors in the early and late part of the curing. This is because the measurement does not display much of a left-side tail before the exotherm and has a long tail to the right side of the exotherm (Figure 4).

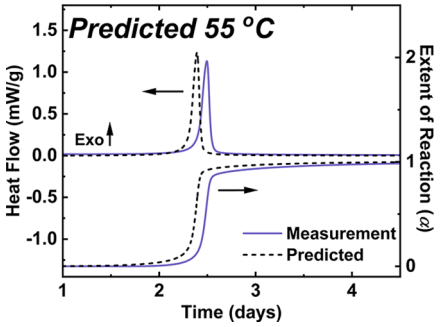

Figure 4. Measured and predicted heat flow (y-axis left) and extent of reaction (y-axis right) of LL50 curing at 55 °C.

This shape is unique compared to the measurements conducted at other temperatures. In respect to interpolative capability, we suggest that predicting $t_{0.5}$ within 5% reasonably validates the model (Figure 5).

To evaluate extrapolation to near-room temperature, we compared a simulated isothermal reaction with measurements at 30 °C, as shown in Figure 6. After 16 days and 18 h at 30 °C, one of the samples (Measurement 1) measured a partial heat of cure of −5.15 J/g, corresponding to an extent of reaction (α) of 0.43. Both measurements were halted before a full exothermic peak was completed due to logistical limitations. This result starkly contrasts with the predicted reaction, which was expected to occur after 70 days at 30 °C. So, at least one measurement disagrees with the model by over 50 days for the onset of the exothermic curing peak. The other measurement does not display any kind of significant heat flow acceleration in the time range measured (Measurement 2). For Measurement 1 at 30 °C, the model significantly overestimates the expected time to react. We struggle to explain this mechanistically besides to conclude that the model is limited in

https://doi.org/10.1021/acsomega.4c09881
ACS Omega 2025, 10, 10294−10301

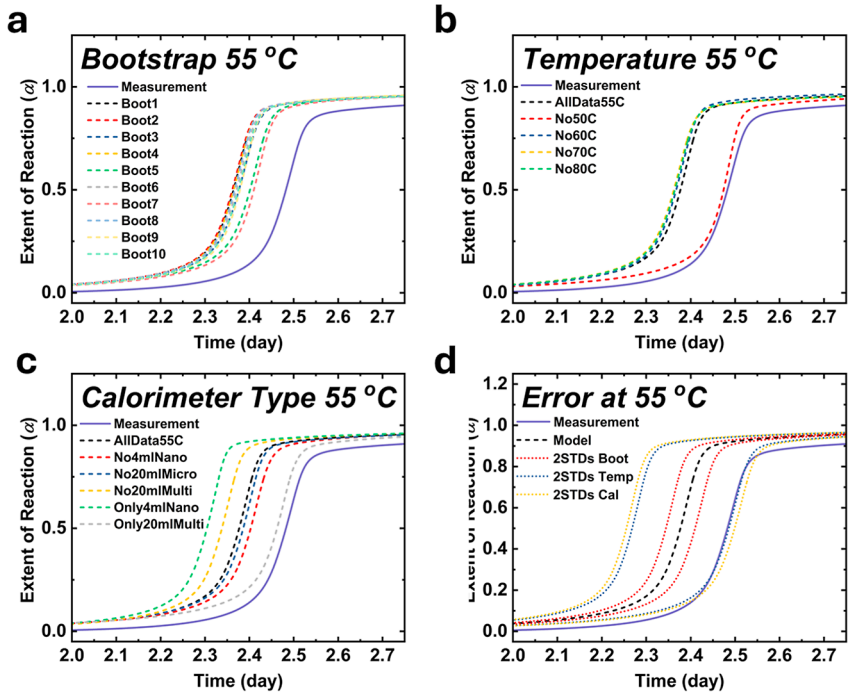

Figure 5. Simulations of LL50 curing at 55 °C using a (a) Monte Carlo Bootstrap analysis, (b) simulations excluding one temperature of measurement, (c) simulations excluding calorimeter types, and (d) estimated error from each analysis.

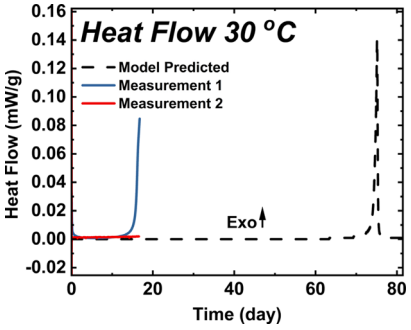

Figure 6. Heat flow from isothermal calorimetry measurement of a partial cure and fitted parameters of LL50 curing at 30 °C.

its ability to extrapolate to lower temperatures than used for the model. It is important to note that Measurement 1 was mixed in mid-November 2023 and was used in the measurements of 50, 60, 70, and 80 °C over the course of 8 weeks. By necessity, the sample was exposed to room temperature during preparation of other experiments for hours at a time. Otherwise, the material was stored in a freezer (∼0 °C) until the 30 °C measurements were performed in June 2024. Still, even if you generously assume 1 day of room temperature exposure for each day of preparation, it does not sum to be more than 1 week. Measurement 2 was prepared in mid-December 2023 and was exposed to less room temperature. Both samples were stored in the same freezer. If we use the model to predict curing in a freezer (0 °C) for 6−7 months, a result of $\alpha = \sim 0.0001$ is returned. So, from the model, there should have been almost no curing occurring during freezer storage. However, as evidenced from Measurement 1, there is clearly curing occurring on an advanced timeline compared to expectations. It is unclear what this change in curing behavior is a result from.

It is fair to conclude that the model fails to extrapolate to near-room temperature for at least one of the measurements. Possible explanations for this discrepancy might include different mechanisms controlling cross-linking at lower temperatures than the high temperatures investigated in this study and in literature.[28−30] Isoconversional methods are developed on the basis that the reaction rate is dependent only on temperature at a constant extent of reaction. Isoconversional methods do not account for influences on the reaction rate that may not be dependent on temperature or which may influence the reaction nonproportionally. The data show that the actual rate of reaction is faster at lower temperatures than expected by the model. Practical application of the kinetic model should be limited to use within the range of 50 to 80 °C. We cannot definitively assess the model's accuracy outside of the specified range, except at 30 °C. However, we can hypothesize that the model may exhibit poor agreement at temperatures below 30 °C. Within the range of 30 to 50 °C, we anticipate that the model's accuracy will improve as the temperature approaches 50 °C, while it is likely to be less accurate closer to 30 °C. Nonetheless, we are unable to ascertain whether this relationship is linear or follows a different pattern. We speculate that the faster reaction rate evidenced by Measurement 1 at 30 °C could be due to the influence of diffusion on our system. LL50 precursor is a viscous polymer. The activation energy of diffusivity does not necessarily scale similarly to the cross-linking reaction with the temperature. At lower temperatures, diffusion limitations may be neglected as mass transport resistance is insignificant over the timescales of the reaction evidenced here. However, at high temperatures, such as those used to feed our model, diffusion limitations may exhibit a greater influence on the measured reaction rate. Regardless, the disagreement observed highlights an important, and often ignored, practice of validating a kinetic model that was derived in a thermal environment different than the conditions of interest. Data are usually collected in

https://doi.org/10.1021/acsomega.4c09881
ACS Omega 2025, 10, 10294−10301

convenient thermal environments such as the fast dynamic measurements of a DSC or high isothermal temperatures because it shortens the time of measurements. Often, the derived models at higher temperatures and fast reaction rates extrapolate well to other thermal environments, and validation reinforces confidence. But, as exemplified here, outside the thermal environments tested, predictions can differ significantly because of the interplay of chemical reaction kinetics, diffusion mechanisms, and physicochemical properties. For the most confidence in predictions, models should be derived with data collected under conditions close to the environment of interest when possible. This may require long measurement times and may not be feasible in a laboratory setting with instruments in high demand or may be limited by the sensitivity of the instruments. There is clearly a balance to be struck.

The kinetics derived provide a guide for the processing of LL50 within the temperature regions measured. In practice, LL50 may be stored and processed at variable temperatures that may be influenced by numerous nonisothermal heat sources including mechanical stirring during two-part mixing, 3D printing machinery, and environmental conditions. The curing may be diffusion limited at higher temperatures and reaction limited at near-room temperatures. Any additional source of heat may increase the rate of the reaction. Furthermore, the study highlights the utility of isothermal HFC and provides an example of how kinetic models may fail validation experiments.

CONCLUSIONS

This study monitored the thermal behavior and modeled the kinetics of curing of LL50, a PDMS-based polymer, by using isothermal HFC. The kinetic model developed was validated within the temperature range of 50 to 80 °C, demonstrating its utility in predicting the curing behavior of LL50 under these conditions. However, the model's extrapolation to near-room temperatures (30 °C) revealed significant discrepancies, suggesting that different mechanisms may govern the curing process at lower temperatures. This finding underscores the necessity of validating kinetic models across the full range of relevant temperatures to ensure accurate predictions. The kinetic model provides a valuable tool for optimizing processing conditions, although it should be used with caution, particularly at temperatures outside the validated range. Overall, this research demonstrates the effectiveness of isothermal calorimetry in studying the curing behavior of PDMS-based polymers and provides a framework for evaluating the rates of curing of other polymer systems.

ASSOCIATED CONTENT

Supporting Information

The Supporting Information is available free of charge at https://pubs.acs.org/doi/10.1021/acsomega.4c09881.

Technical information on calorimetry measurements, thermogravimetric analysis of LL50 curing, integration and fits of calorimetric data, integrated heat of cure vs mass of sample, integrated heat of cure vs temperature of measurement, and bootstrap sampling (PDF)

AUTHOR INFORMATION

Corresponding Author

Cody Cockreham − *Materials Science Division, Lawrence Livermore National Laboratory, Livermore, California 94550, United States;* orcid.org/0000-0002-8740-2197; Email: cockreham1@llnl.gov

Authors

John Rosener − *Materials Science Division, Lawrence Livermore National Laboratory, Livermore, California 94550, United States;* orcid.org/0009-0001-6673-3691

Steven A. Hawks − *Materials Science Division, Lawrence Livermore National Laboratory, Livermore, California 94550, United States;* orcid.org/0000-0002-5983-8698

Elizabeth Glascoe − *Materials Science Division, Lawrence Livermore National Laboratory, Livermore, California 94550, United States*

Complete contact information is available at: https://pubs.acs.org/10.1021/acsomega.4c09881

Notes

The authors declare no competing financial interest.

ACKNOWLEDGMENTS

We thank Jeremy A. Armas, Andrew D. Alexopoulos, and Laural Hargrove at LLNL for providing and mixing LL50. We thank Jeremy Lenhardt at LLNL for his comments and suggestions. This work was performed under the auspices of the U.S. Department of Energy by Lawrence Livermore National Laboratory under Contract DE-AC52-07NA27344.

REFERENCES

(1) Miranda, I.; Souza, A.; Sousa, P.; Ribeiro, J.; Castanheira, E. M. S.; Lima, R.; Minas, G. Properties and Applications of PDMS for Biomedical Engineering: A Review. *J. Funct. Biomater.* **2022**, *13* (1), 2.

(2) Raj M, K.; Chakraborty, S. PDMS Microfluidics: A Mini Review. *J. Appl. Polym. Sci.* **2020**, *137* (27), 48958.

(3) Qi, D.; Zhang, K.; Tian, G.; Jiang, B.; Huang, Y. Stretchable Electronics Based on PDMS Substrates. *Adv. Mater.* **2021**, *33* (6), 2003155.

(4) Ribeiro, J.; Lima, R. Applications of Polydimethylsiloxane (PDMS) in Engineering. *Encyclopedia* **2022**.

(5) Stevens, C.; Powell, D. E.; Mäkelä, P.; Karman, C. Fate and Effects of Polydimethylsiloxane (PDMS) in Marine Environments. *Mar. Pollut. Bull.* **2001**, *42* (7), 536−543.

(6) Bridges, A. J. Silicone Breast Implants: History, Safety, and Potential Complications. *Arch. Int. Med.* **1993**, *153* (23), 2638.

(7) Alkhalaf, Q.; Pande, S.; Palkar, R. R. Review of Polydimethylsiloxane (PDMS) as a Material for Additive Manufacturing. In *Innovative Design, Analysis and Development Practices in Aerospace and Automotive Engineering*; Gascoin, N., Balasubramanian, E., Eds. Lecture Notes in Mechanical Engineering; Springer Singapore: Singapore, 2021; pp 265−275..

(8) Tony, A.; Badea, I.; Yang, C.; Liu, Y.; Wells, G.; Wang, K.; Yin, R.; Zhang, H.; Zhang, W. The Additive Manufacturing Approach to Polydimethylsiloxane (PDMS) Microfluidic Devices: Review and Future Directions. *Polymers* **2023**, *15* (8), 1926.

(9) Lenhardt, J. *Llama 20, 40, 50 and 60 Siloxanes for Direct Ink Write − Compositional Information*; Lawrence Livermore National Lab.(LLNL): Livermore, 2022; p 1871381..

(10) Durban, M. M.; Lenhardt, J. M.; Wu, A. S.; Small, W.; Bryson, T. M.; Perez-Perez, L.; Nguyen, D. T.; Gammon, S.; Smay, J. E.; Duoss, E. B.; Lewicki, J. P.; Wilson, T. S. Custom 3D Printable Silicones with Tunable Stiffness. *Macromol. Rapid Commun.* **2018**, *39* (4), 1700563.

(11) Sharma, H. N.; Lenhardt, J. M.; Loui, A.; Allen, P. G.; McLean, W.; Maxwell, R. S.; Dinh, L. N. Moisture Outgassing from Siloxane Elastomers Containing Surface-Treated-Silica Fillers. *Npj Mater. Degrad.* **2019**, *3* (1), 21.
(12) Van Meerbeek, I. M.; Lenhardt, J. M.; Small, W.; Bryson, T. M.; Duoss, E. B.; Weisgraber, T. H. Compressive Properties of Silicone Bouligand Structures. *MRS Bull.* **2023**, *48* (4), 325−331.
(13) Sturgess, C.; Tuck, C. J.; Ashcroft, I. A.; Wildman, R. D. 3D Reactive Inkjet Printing of Polydimethylsiloxane. *J. Mater. Chem. C* **2017**, *5* (37), 9733−9743.
(14) Llorente, M. A.; Mark, J. E. Model Networks of End-Linked Poly(Dimethylsiloxane) Chains. 8. Networks Having Cross-Links of Very High Functionality. *Macromolecules* **1980**, *13* (3), 681−685.
(15) Venkataraman, S. K.; Coyne, L.; Chambon, F.; Gottlieb, M.; Winter, H. H. Critical Extent of Reaction of a Polydimethylsiloxane Polymer Network. *Polymer* **1989**, *30* (12), 2222−2226.
(16) Young, R. J.; Lovell, P. A. *Introduction to Polymers*; CRC Press, 2011; ..
(17) Vyazovkin, S.; Sbirrazzuoli, N. Isoconversional Kinetic Analysis of Thermally Stimulated Processes in Polymers. *Macromol. Rapid Commun.* **2006**, *27* (18), 1515−1532.
(18) AKTS-Thermokinetics Software and AKTS-Thermal Safety Software. www.akts.com.
(19) Deshpande, G.; Rezac, M. E. Kinetic Aspects of the Thermal Degradation of Poly(Dimethyl Siloxane) and Poly(Dimethyl Diphenyl Siloxane). *Polym. Degrad. Stab.* **2002**, *76* (1), 17−24.
(20) García-Garrido, C.; Pérez-Maqueda, L. A.; Criado, J. M.; Sánchez-Jiménez, P. E. Combined Kinetic Analysis of Multistep Processes of Thermal Decomposition of Polydimethylsiloxane Silicone. *Polymer* **2018**, *153*, 558−564.
(21) Stein, J.; Lewis, L. N.; Gao, Y.; Scott, R. A. In Situ Determination of the Active Catalyst in Hydrosilylation Reactions Using Highly Reactive Pt(0) Catalyst Precursors. *J. Am. Chem. Soc.* **1999**, *121* (15), 3693−3703.
(22) Lewis, L. N.; Uriarte, R. J. Hydrosilylation Catalyzed by Metal Colloids: A Relative Activity Study. *Organometallics* **1990**, *9* (3), 621−625.
(23) Petrucci, R. H. *General Chemistry: Principles and Modern Applications*, 9 ed.; Pearson/Prentice Hall: Upper Saddle River, N.J, 2007.
(24) Atkins, P. W.; Ratcliffe, R. G.; Wormald, M. R.; De Paula, J. *Physical Chemistry for the Life Sciences*; Oxford University Press: New York, NY, 2023
(25) Roduit, B.; Folly, P.; Sarbach, A.; Berger, B.; Brogli, F.; Mascarello, F.; Schwaninger, M.; Glarner, T.; Irle, E.; Tobler, F. Estimation of Time to Maximum Rate under Adiabatic Conditions (TMRad) Using Kinetic Parameters Derived from DSC-Investigation of Thermal Behavior of 3-Methyl-4-Nitrophenol. *Chem. Propel Polym. Mater.* **2011**, *1*, 84−93.
(26) Zsakó, J. The Kinetic Compensation Effect. *J. Therm. Anal. Calorim.* **1976**, *9* (1), 101−108.
(27) Esteves, A. C. C.; Brokken-Zijp, J.; Laven, J.; Huinink, H. P.; Reuvers, N. J. W.; Van, M. P.; De With, G. Influence of Cross-Linker Concentration on the Cross-Linking of PDMS and the Network Structures Formed. *Polymer* **2009**, *50* (16), 3955−3966.
(28) Hong, I.-K.; Lee, S. Cure Kinetics and Modeling the Reaction of Silicone Rubber. *J. Ind. Eng. Chem.* **2013**, *19* (1), 42−47.
(29) Harkous, A.; Colomines, G.; Leroy, E.; Mousseau, P.; Deterre, R. The Kinetic Behavior of Liquid Silicone Rubber: A Comparison between Thermal and Rheological Approaches Based on Gel Point Determination. *React. Funct. Polym.* **2016**, *101*, 20−27.
(30) Bardelli, T.; Marano, C.; Briatico Vangosa, F. Polydimethylsiloxane Crosslinking Kinetics: A Systematic Study on Sylgard184 Comparing Rheological and Thermal Approaches. *J. Appl. Polym. Sci.* **2021**, *138* (39), 51013.

https://doi.org/10.1021/acsomega.4c09881
ACS Omega 2025, 10, 10294−10301